

# Robust Data Acquisition for MR Doppler

D. Lee<sup>1</sup>, A. B. Kerr<sup>1</sup>, J. M. Santos<sup>2</sup>, B. S-C. Hu<sup>3</sup>, and J. M. Pauly<sup>1</sup>

<sup>1</sup>Electrical Engineering, Stanford University, Stanford, CA, United States, <sup>2</sup>HeartVista, Inc., Palo Alto, CA, United States, <sup>3</sup>Cardiology, Palo Alto Medical Foundation, Palo Alto, CA, United States

**INTRODUCTION:** The pressure gradient across cardiac valves is commonly utilized to evaluate the severity of valvular stenosis. Peak velocity is often used to derive the pressure-gradient, and more accurate estimation is possible with a localized velocity spectrum. MR Doppler has been shown to effectively acquire a spatially resolved velocity spectrum in real-time without cardiac gating thanks to resolving flow along a cylindrical pathway restricted by pencil beam excitation [1-4]. The fidelity of velocity estimation is especially critical for diagnosing stenotic flow in the range of 2-3 m/s. However, off-resonance, inflow effect, and flow acceleration during readout incurs signal drop and spurious dispersion in the velocity spectrum, degrading the velocity estimation. We present a circular  $k$ -space echo-shifted interleaved acquisition method to improve the reliability of velocity estimation, especially for imaging high-velocity jets.

**THEORY:** A large FOV<sub>v</sub> requirement for detecting high-speed jets results in a longer echo time (TE) and readout time (T<sub>DAQ</sub>) and a cruder spatial resolution ( $\Delta z$ ) for a desired velocity resolution ( $\Delta v$ ). However, TE must be kept short to avoid signal dephasing due to flow acceleration, and shorter T<sub>DAQ</sub> reduces sensitivity to off-resonance induced artifacts (e.g., velocity shift and signal dephasing). In this regard, an interleaved readout [5,6] is more promising than a simple variable-density approach [4] in the sense that it not only reduces the amount of velocity shifting (due to shorter TE) and T<sub>DAQ</sub> but also improves the spatial resolution as each interleaf is fundamentally a smaller FOV<sub>v</sub> readout.

Starting from the geometric perspective, a circular  $k$ -space sampling method is adopted to increase the utilization of acquired data as it achieves a more uniform distribution by shifting spokes in  $k_z$  direction. Further improvement on the sampling efficiency is obtained with the variable-density approach to achieve a more uniform and efficient  $k$ -space sampling. Finally, TE and T<sub>DAQ</sub> were reduced by adopting the interleaved approach. When designing interleaves, each readout is deliberately delayed after the prewinder to make the phase transition smoother in  $k$  space. This not only reduces the ghosting artifacts, coming from off-resonance and T<sub>2</sub> decay [6], but also improves the uniformity of  $k$ -space sampling, resulting in suppressed sidelobes.

**METHODS:** As summarized in Table 1, three representative readout gradient waveforms; square uniform 1-shot (SU1), circular variable 1-shot (CV1) and circular variable 3-shot (CV3) were designed with the method in Ref. [7] to resolve the casual 4-m/s stenotic peak velocity assuming a maximum gradient amplitude of 40 mT/m, maximum slew rate of 150 T/m/s, and a sampling time of 4  $\mu$ sec. All three sequences were verified with PSF simulations as shown in Fig. 1. All experiments were performed on the RTHawk real-time interactive MRI system [8,9], which is interfaced to a GE Signa 1.5 T scanner (GE Healthcare, Milwaukee, WI, USA). The spatial direction is first aligned to the flow direction with careful shimming. Then, MR Doppler acquisitions were performed exclusively with its maximum temporal resolution for the same imaging geometry. While the space-velocity ( $z$ - $v$ ) images were reconstructed in real-time, time-velocity ( $t$ - $v$ ) images were compiled at desired spatial locations by adjusting a control slider on the real-time system. A flow phantom was constructed to simulate stenotic aortic blood flow: a tube with 12.7-mm diameter was connected to a pulsatile blood pump for animals and jet-flow was simulated at the nozzle of an area reducer (from 12.7 mm to 9.5 mm) in the middle of tube.

**RESULTS AND DISCUSSION:** Signal losses are observed near the area reducer due to the susceptibility artifacts on the pump-off images in Fig. 2. Also, the off-resonance-induced velocity shifts are easily discerned. Roughly two times larger velocity shifts were observed with SU1 and CV1 when compared to CV3 due to the difference in the time to traverse  $1/\text{FOV}_v$  along  $k_z$ . For the pulsatile flow experiments,  $v$ - $t$  images were compiled at two spatial locations, downstream ( $z = A$ ) and upstream ( $z = B$ ) of the area reducer. The peak velocity is estimated as 3.1 m/s at  $z = A$  and 1.4 m/s at  $z = B$ . All three sequences successfully resolved the pulsatile flow at  $z = A$  where the off-resonance is spatially invariant. In contrast, SU1 and CV1 exhibited significant spurious dispersion at  $z = B$  due to the widely distributed off-resonance in the upstream and this led to an overestimation of peak velocity in both sequences. Note the spurious high-velocity spectrum (indicated with arrows) in SU1's  $t$ - $v$  image where the actual flow reached zero velocity. This was caused by the inflow of the highly off-resonant spins in the upstream. Overall, the circular  $k$ -space echo-shifted interleaved acquisition (i.e., CV3) resulted in the least spurious distribution of velocity, achieving the most consistent velocity spectrum. Though ghosting artifacts were observed in the time frames with high acceleration, this does not degrade the peak-velocity detection capability.

**REFERENCES:** [1] Irarrazabal, P et al., *Magn. Reson. Med.*, 30:207-212 (1993) [2] Luk Pat, GT et al., *Magn. Reson. Med.*, 40:603-613 (1998) [3] MacGowan, CK et al., *J. Magn. Reson. Imag.*, 21:297-304 (2005) [4] DiCarlo, JC et al., *Magn. Reson. Med.*, 54:645-655 (2005) [5] DiCarlo, JC et al., *ISMRM* 11th, 2507 (2003) [6] Kerr, AB et al., *ISMRM* 15th, 2502 (2007) [7] Lee, D et al., *ISMRM* 16th, 1369 (2008) [8] Kerr, AB et al., *Magn. Reson. Med.*, 38:355-367 (1997) [9] Santos, JM et al., *IEEE EMBS* 26th, 1048-1051 (2004)

sequence	SU1	CV1	CV3
sampling shape	square	circle	circle
sampling density	uniform	variable	variable
# of interleaves	1	1	3
$\Delta z$ [cm]	1.5	0.75	0.5
FOV <sub>z</sub> [cm]	59.7	40.2	32.7
T <sub>DAQ</sub> [ms]	18.6	14.6	7.1

**Table 1.** Readout sequences (FOV<sub>v</sub> =  $\pm 425$  cm/s,  $\Delta v \approx 35$  cm/s, and partial  $k$ -space fraction of 0.65 along  $k_z$ ). SU1: conventional method, CV1: circular  $k$ -space single-shot acquisition, CV3: circular  $k$ -space echo-shifted interleaved acquisition.

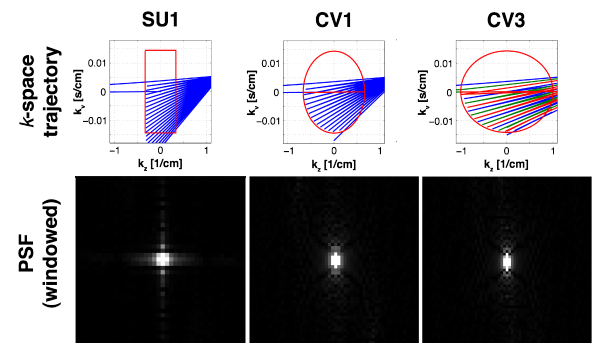


**Figure 1.** Comparison of  $k$ -space trajectories and PSFs (horizontal axis is  $z$ , vertical axis is  $v$ ). All PSFs are windowed between zero and 20% of their maximum intensities. Note that each waveform has a different FOV<sub>z</sub>.

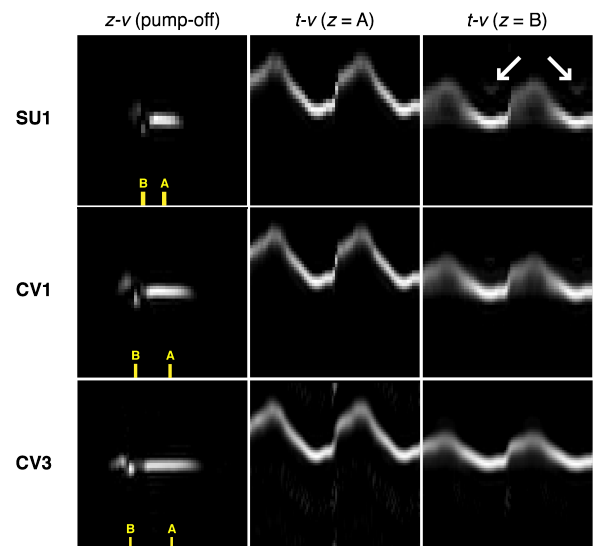


**Figure 2.** Flow phantom experiments. First column shows  $z$ - $v$  images when the pump was turned off. The  $t$ - $v$  images were compiled from the time series of  $z$ - $v$  images at two spatial locations ( $z = A$ ,  $z = B$ ). All images are windowed between 5% and 100% of their maximum intensities.